NASA TECHNICAL NOTE

N73-18002

NASA TN D-7196

NASA TN D-7196

CASE FILE COPY

COMPARISON OF THE AERODYNAMIC CHARACTERISTICS OF AN ABLATING AND NONABLATING BLUNTED CONICAL BODY

by Robert L. Kruse

Ames Research Center
Moffett Field, Calif. 94035

NATIONAL AERONAUTICS AND SPACE ADMINISTRATION • WASHINGTON, D. C. • MARCH 1973

1. Report No.	2. Government Accession No.	3. Recipient's Catalog No.
NASA TN D-7196		

4. Title and Subtitle	5. Report Date
COMPARISON OF THE AERODYNAMIC CHARACTERISTICS OF AN ABLATING AND NONABLATING BLUNTED CONICAL BODY	March 1973
	6. Performing Organization Code
7. Author(s) Robert L. Kruse	8. Performing Organization Report No. A-4558
	10. Work Unit No. 117-07-04-14-00-21
9. Performing Organization Name and Address NASA Ames Research Center Moffett Field, Calif., 94035	11. Contract or Grant No.
	13. Type of Report and Period Covered Technical Note
12. Sponsoring Agency Name and Address National Aeronautics and Space Administration Washington, D. C., 20546	14. Sponsoring Agency Code

15. Supplementary Notes

16. Abstract

The influence of ablation on the aerodynamic characteristics of a blunted slender cone was investigated. Plastic models were launched in free flight at ablating conditions. The results were compared with results of similar tests using metal non-ablating models. Ablation was found to decrease the dynamic stability and the drag, but had little effect on static stability and lift. The plastic models appeared to experience ablation-induced roll.

17. Key Words (Suggested by Author(s))	18. Distribution Statement
Ablation Blunt small-angle cones	Unclassified – Unlimited

19. Security Classif. (of this report)	20. Security Classif. (of this page)	21. No. of Pages	22. Price*
Unclassified	Unclassified	26	$3.00

*For sale by the National Technical Information Service, Springfield, Virginia 22151

SYMBOLS

A	reference area (model base area)
C_D	drag coefficient
C_{L_α}	lift–curve slope
C_{l_o}	rolling–moment coefficient
C_m	pitching–moment coefficient
C_{m_α}	pitching–moment–curve slope
$C_{m_{\alpha_l}}$	quasi–linear pitching–moment–curve slope
$C_{m_q} + C_{m_{\dot{\alpha}}}$	damping–in–pitch derivative, $\dfrac{\partial C_m}{\partial\left(\dfrac{qd}{V}\right)} + \dfrac{\partial C_m}{\partial\left(\dot{\alpha}\,\dfrac{d}{V}\right)}$
d	model base diameter
I_y	moment of inertia about a transverse axis through the center of gravity
I_x	moment of inertia about the roll axis
l	model length
M	Mach number
m	model mass
$\dot{m}$	total mass–loss rate
$\dfrac{\dot{m}}{\rho VA}$	ablation parameter (steady state)
p	roll rate about model axis of symmetry
q	angular pitching velocity
Re	Reynolds number based on free–stream conditions and model base diameter
r_b	model base radius
r_n	model nose radius

T	free–stream temperature
t	time
V	free–stream velocity
$X_{c.g.}$	axial distance from model nose to center of gravity
x	distance flown
y	horizontal range coordinate perpendicular to x and z axes
z	vertical range coordinate perpendicular to x and y axes
α	angle of attack (in the vertical plane)
β	angle of sideslip (in the horizontal plane)
θ	cone half–angle
λ	wavelength of pitching oscillation
μ	viscosity
ξ	dynamic stability parameter
ρ	free–stream air density
σ	resultant angle of attack, $\tan^{-1}(\tan^2\alpha + \tan^2\beta)^{1/2}$
σ_m	average maximum resultant angle of attack
$\sigma_{\min}$	average minimum resultant angle of attack
σ_{rms}	root–mean–square resultant angle of attack, $\left(\frac{\int_o^x \sigma^2 dx}{x}\right)^{1/2}$
ω_1, ω_2	rate of rotation of vectors that describe the model oscillatory motion in equation (3)
$\frac{\omega d}{V}$	reduced frequency parameter
$(\dot{\ })$	first derivative with respect to time

COMPARISON OF THE AERODYNAMIC CHARACTERISTICS OF AN ABLATING AND NONABLATING BLUNTED CONICAL BODY

Robert L. Kruse

Ames Research Center

SUMMARY

The influence of ablation on the aerodynamic characteristics of a blunted slender cone was investigated. Plastic models were launched in free flight at ablating conditions. The results were compared with results of similar tests using metal nonablating models. Ablation was found to decrease the dynamic stability and the drag, but had little effect on static stability and lift. The plastic models appeared to experience ablation-induced roll.

INTRODUCTION

In the past, a number of investigations have been conducted to determine the influence of ablation on the aerodynamic characteristics of slender cones (ref. 1). These investigations were motivated by unexplained flight results of full-scale entry vehicles. The present investigation evolved as a result of flights during which the vehicles exhibited dynamic instabilities during a portion of the entry. It was suspected that ablation from the surface of the vehicle interacted with the boundary layer, thereby altering the aerodynamic characteristics which resulted in the observed instabilities.

The feasibility of utilizing a ballistic range to investigate the effect of ablation is discussed in reference 1. The present investigation was undertaken in an attempt to contribute to the understanding of the effects of ablation on the aerodynamics of slender bodies.

MODEL AND SABOTS

Figure 1 is a sketch of the configuration used in the present investigation. The models were 6° half-angle cones with a bluntness $r_n/r_b = 0.31$. The bases were hollowed to obtain the desired center-of-gravity position. The models for the ablation tests were made of delrin, those for the nonablation tests, of bimetallic construction. The nose, rearward to the tangent point, was tantalum press-fitted into the aluminum afterbody.

The models were encapsulated by the sabot except for the spherical nose. A completely encapsulated model would not launch successfully. It was suspected that the sabot fingers hung up on the model nose and upset it during separation.

TEST CONDITIONS

The test conditions necessary for ablation were analyzed using the method for a pointed cone described in reference 1 and discussed further in reference 2. To apply this method to the blunted cone of this study, it was necessary to consider the differences in surface heat transfer between pointed and blunted cones. These differences were accounted for utilizing the data presented in reference 3. From the results presented there, it was determined that for a cone, blunted the amount of the present one, the heat transfer over the body averaged about 85 percent of that for a pointed cone.

In reference 2, lexan, teflon, and delrin were found to be the most suitable commercially available plastics for ablation studies in ballistic ranges. Calculations made for the present tests indicate that delrin was the best suited because it achieved a given ablation rate at the lowest velocity. The ablation rate at the model base was 80 percent of the steady-state value; for steady state, $\dot{m}/\rho VA = 0.01$.

The models were launched from a deformable-piston light-gas gun with a bore diameter of 2.5 mm. Shadowgraphs were taken in orthogonal planes at 16 observation stations for a ballistic flight of 23 m. The ambient pressure was 76 mm Hg, and the Reynolds number was nominally 300,000 based on free-stream conditions and model base diameter.

DATA REDUCTION

The data-reduction techniques used to obtain the aerodynamic coefficients of drag, lift, and static and dynamic stability from free-flight data are presented in reference 4. In this section, only the basic equations and a brief description of the techniques used will be presented.

Drag

Drag coefficients were obtained from the flight time and distance measurements by the method presented in reference 4, which assumes a constant drag coefficient. The equation relating time and distance is written:

$$t = t_o - \frac{1}{V_o k C_D} + \frac{e^{kC_D x}}{V_o k C_D} \tag{1}$$

where V_o and t_o are velocity and time at $x = 0$ and $k = \rho A/2m$. The parameters C_D, V_o, and t_o are determined to give the "best fit" in the least squares sense to the measured values of x and t. A method applicable to cases in which the drag coefficient varies with angle of attack is presented in reference 5. The drag coefficient was shown to vary with the resultant angle of attack according to the relation:

$$C_D = C_{D_o} + C_{D_2}\sigma^2 \tag{2}$$

The effective drag coefficient obtained from equation (1) is the drag coefficient that would be obtained at a constant angle of attack equal to the root-mean-square resultant angle of attack of a given flight. The present results were found to be represented adequately by equation (2), as will be shown.

Static and Dynamic Stability Derivatives

The stability derivatives were determined from analysis of the pitching and yawing motions experienced by the models during free flight. The analysis consisted in fitting the following tricyclic equation, derived by Nicolaides (ref. 6), to the measurements of α and β of each flight:

$$\beta + i\alpha = K_1 e^{(\eta_1 + i\omega_1)x} + K_2 e^{(\eta_2 - i\omega_2)x} + K_3 e^{ipx} \tag{3}$$

where $\eta_{1,2}$ and $\omega_{1,2}$ are functions of the aerodynamic stability coefficients and $K_{1,2,3}$ are functions of the initial conditions. The most important assumptions inherent in this equation are linear aerodynamics, small angles of attack, constant roll rate, and small asymmetries. In the present analysis, the Magnus moment was assumed to be zero. A least-squares procedure using differential corrections was used to determine optimum values of the constants.

The static and dynamic stability parameters are related to the constants in equation (3) as follows. The wavelength of the oscillation is given by

$$\lambda = 2\pi/(\omega_1 \omega_2)^{1/2} \tag{4}$$

The pitching-moment-curve slope, C_{m_α}, is computed from

$$C_{m_\alpha} = -8\pi^2 I_y/\lambda^2 \rho A d \tag{5}$$

The dynamic stability parameter, ξ, defined as

$$\xi = C_D - C_{L_\alpha} + (C_{m_q} + C_{m_{\dot\alpha}})(d^2 m/I_y) \tag{6}$$

is determined from the constants η_1 and η_2 by means of

$$\xi = (\eta_1 + \eta_2)/(\rho A/2m) \tag{7}$$

It has been shown (refs. 7 and 8) that ξ is a measure of the dynamic stability of a vehicle both in unpowered flight at constant altitude and in ballistic entry.

Although the assumption of linear aerodynamics is inherent in equation (3), this does not prevent its use for bodies with nonlinear static stability coefficients. Each individual flight is reduced as if the governing pitching moment were linear with angle of attack. The resulting wavelength of oscillation represents a quasi-linear value for the pitching-moment-curve slope or static stability. Quasi-linear values for static stability from several flights at various angle-of-attack amplitudes can be used to obtain the nonlinear pitching-moment coefficient as a function of angle of attack. The method is derived in reference 9 and illustrated in some detail in reference 10. This method uses values for $C_{m_{\alpha_l}}$, σ_m, and $\sigma_{\min}$ to produce an expression in C_m versus σ. Its validity depends on the assumption that interactions between static and dynamic terms are negligibly small.

Lift

The lift-curve slope, C_{L_α}, was obtained for each flight by analyzing the swerving motion of the model, in conjunction with the oscillatory motion of the model given by equation (3). A modified form of Nicolaides' equation is fitted by the method of least squares to the measured displacement data y and z:

$$y + iz = -\frac{\rho A}{2m}\left[C_{L_\alpha}\int_o^x\int_o^x(\beta + i\alpha)dx\,dx + \left(C_{y_o} + iC_{L_o}\right)\left(\frac{1 + ipx - e^{-ipx}}{p^2}\right)\right] + (y_o' + iz_o')x + (y_o + iz_o) \tag{8}$$

The constants C_{y_o} and C_{L_o} are necessary to account for small model asymmetries. For a carefully machined body of revolution, they will be negligibly small.

The nonlinear lift coefficient can be derived as a function of angle of attack by using an approximate method similar to that described for the pitching moment with C_{L_α} substituted for $C_{m_{\alpha_l}}$.

RESULTS AND DISCUSSION

The model characteristics and test conditions are given in table 1 along with the data reduced from the tests.

Model Motions

Typical model motions are presented in figure 2, where the angle of attack, α, is plotted versus the angle of sideslip, β. The circles are the measured data points, and the machine fit of the equation of motion (eq. (3)) to the data points is shown. A typical nonablating model motion (fig. 2(a)) is seen to be regular (i.e., the character of each cycle is repeated) and to have experienced little roll. A typical motion of an ablating model is shown in figure 2(b). Its motion also is regular, as were the other ablating models in these tests, in contrast to the results reported in reference 2. The ablating models as a group experienced more roll than the nonablating models (see table 1). It is felt that this must be a result of ablation. The influence of ablation on roll is reported in reference 11. However, the induced roll (ref. 11) was thought to result from the cross-hatching, which occurs only under turbulent boundary layers. In the present tests, the boundary-layer flow is laminar as shown by the shadowgraphs in figure 3. The laminar flow over the model is inferred by the extensive laminar wake. Therefore, the induced roll in the present ablation tests must have resulted from some other source, such as local surface distortion caused by asymmetric ablation.

Drag

The drag coefficient, C_D, is presented as a function of the mean-square resultant angle of attack in figure 4. Least-square lines through the ablation and no-ablation data correlate the data, consistent with equation (2), as previously mentioned. From a comparison of the data, the results of the ablation tests indicate a slight but consistent decrease in C_D throughout the angle-of-attack range. Similar results are reported in reference 2. Calculated components of the drag coefficient for zero angle of attack are also shown in figure 4. The wave drag was determined by a method developed at Ames Research Center by John V. Rakich. Estimates of the remaining components (skin friction, base drag, viscous interaction) were made, assuming both no ablation and steady-state ablation. The required heat-transfer and skin-friction calculations depended heavily on the boundary-layer program described in reference 12 modified to include blowing at the wall. These calculated values are in good agreement with those obtained by extrapolation of the experimental data to $\sigma = 0°$. The differences in C_D between the nonablating and ablating models are largely a result of the reduction in skin friction due to ablation. Therefore, it was felt that near steady-state ablation did, in fact, occur on the plastic models in the present investigation. The drag coefficient versus resultant angle of attack obtained from the least-square fit of the drag data (fig. 4) is shown in figure 5.

Static Stability

The static stability results are presented in figure 6, where the quasi-linear static stability parameter $C_{m_{\alpha_l}}$ is plotted as a function of σ_m. In general, $C_{m_{\alpha_l}}$ increases with σ_m throughout the σ_m range for both ablation and nonablation. There is little effect of ablation in contrast to that found for a pointed cone (ref. 2), where ablation reduced C_{m_α}. Extrapolating the data to $\sigma_m = 0$ shows poor agreement with the Newtonian estimate for C_{m_α} (indicated by N) while agreement with the Rakich estimate (indicated by R) appear fairly good.

The values of $C_{m_{\alpha_l}}$ from the tests were used to determine C_m as a function of σ. The expression for the ablating case is

$$C_m = 0.00642\sigma - 0.00288\sigma^2 + 0.000105\sigma^3$$

For the nonablating case

$$C_m = -0.00310\sigma - 0.00107\sigma^2 + 0.0000325\sigma^3$$

(see fig. 7). Within the angle range tested, the nonablating configuration is stable while the ablating configuration appears unstable below about 3°. The curve for the ablating configuration indicates that a trim point exists near 3° angle of attack. However, none of the motion histories indicate that the models flew at trim angles other than 0°. The method of constructing the C_m versus σ curve is not of sufficient accuracy to allow more than an inference that the slope of the curve near $\sigma = 0$ is markedly reduced in the presence of ablation.

Lift

The lift–curve slope, C_{L_α}, given in figure 8 as a function of σ_m, is nonlinear and increases with σ_m. There is very little difference between the ablation and nonablation results. The Newtonian theory estimate is high while the Rakich estimate compares favorably with an extrapolated value.

Expressions were obtained for C_L as a function of σ using the previously explained method. For the ablating case:

$$C_L = -0.00768\sigma + 0.00452\sigma^2 - 0.000132\sigma^3$$

For the nonablating case,

$$C_L = 0.00815\sigma + 0.00217\sigma^2 - 0.000052\sigma^3$$

(see fig. 9). The ablating model appears to have negative lift at angles of attack between 0° and 2°; above 2°, it approaches the nonablation result. As mentioned previously, this method of curve construction may only allow an inference that the slope of the curve in the vicinity of $\sigma = 0$ is reduced in the presence of ablation.

Normal Force

The relationship between normal force and angle of attack (fig. 10) was determined from the measured lift and drag data for $C_N = C_L \cos \sigma + C_D \sin \sigma$. There is little difference between the ablation and nonablation cases.

Dynamic Stability

The damping-in-pitch derivative, $C_{m_q} + C_{m_{\dot{\alpha}}}$, is shown as a function of σ_m in figure 11. For the nonablating case, the results indicate that the configuration is stable with the stability increasing with σ_m. The value from Newtonian theory is indicated by a tick labeled N and falls in line quite well with the experimental results. The effect of ablation is to decrease the dynamic stability, and results in a dynamically unstable configuration below about 6°.

These differences in the ablation and nonablation results are unlike those found using a pointed cone in reference 2, where the configuration was stable for both cases with no significant difference in the level of stability between the two.

Care must be taken when analyzing dynamic stability data with a quasi-linear data-reduction procedure. In reference 13, it was shown that the presence of nonlinear static stability can greatly alter the apparent dynamic stability. Hence, while the large decrease in dynamic stability due to ablation is real (both nonablating and ablating models have the same nonlinearities in C_m), the absolute values of $C_{m_q} + C_{m_{\dot{\alpha}}}$ and the trends with angle of attack may be misleading. It is possible that incorporating a nonlinear moment system (e.g., such as that proposed in ref. 14) in the data reduction procedure would eliminate this deficiency.

Rolling Moment

It was stated previously that the roll rate, p, experienced by the plastic ablating models was greater as a group than that experienced by the metal nonablating models. From these data, a rough estimate was made of the metal nonablating models. From these data, a rough estimate was made of the ablation-induced rolling moment coefficient, C_{l_o}. The absolute values of roll rates were averaged for the two cases, those from the nonablating tests were assumed to be gun-induced, and the difference between the two cases was considered to be due to ablation. The rolling moment was determined from

$$\text{Rolling moment} = I_x \dot{p}$$

The roll acceleration of the model, $\dot{p}$, was determined assuming that $\dot{p}$ was constant from the gun muzzle and

$$\dot{p} = \frac{pV}{x}$$

where x is the distance from the gun muzzle to the test section midpoint and V, the model velocity. With these considerations, the rolling moment coefficient, C_{l_o}, was estimated to be 0.003, considerably greater than the values of 10^{-4} to 10^{-5} from tests using 15° and 30° half-angle pointed cones at $M = 7.4$ (ref. 11).

CONCLUSION

The results of the investigation show that both ablating and nonablating models experienced fully laminar flow and that, within the angle range tested, ablation affected the aerodynamic characteristics in the following manner:

1. The dynamic stability was greatly reduced. An instability may exist at small angles of attack. The test data are difficult to interpret because of unassessed assumptions in aerodynamic moment formulation.

2. The drag coefficient was reduced by approximately 6 percent, most of which can be ascribed to a reduction in skin friction.

3. The pitching moment appeared to change only a small amount with ablation; however, the ablating models did indicate a reduction in slope of the pitching-moment curve near 0° angle of attack. In both cases, the pitching moment was nonlinear with angle of attack.

4. The ablating models experienced considerable induced roll. The reason for this is unknown.

5. Lift and normal forces were found to be nonlinear for both the ablation and nonablation cases and changed very little with ablation.

Ames Research Center
National Aeronautics and Space Administration
Moffett Field, Calif., 94035, September 8, 1972

REFERENCES

1. Kirk, Donn B.; Intrieri, Peter I.; and Terry, James E.: Ablation Testing in Ballistic Ranges. AIAA Paper 69–385, 1968.

2. Intrieri, Peter F.; Kirk, Donn B.; Chapman, Gary T.; and Terry, James E.: Ballistic Range Tests of Ablating and Nonablating Slender Cones. AIAA Paper 69–179, 1969.

3. Wilkinson, David B.; and Harrington, Shelby A.: Hypersonic Force, Pressure, and Heat Transfer Investigations of Sharp and Blunt Slender Cones. AEDC–TDR–63–177, Aug. 1963.

4. Malcolm, Gerald N.; and Chapman, Gary T.: A Computer Program for Systematically Analyzing Free-Flight Data to Determine the Aerodynamics of Axisymmetric Bodies. NASA TN D–4766, 1968.

5. Seiff, Alvin; and Wilkins, Max E.: Experimental Investigation of a Hypersonic Glider Configuration at a Mach Number of 6 and at Full-Scale Reynolds Numbers. NASA TN D–341, 1961.

6. Nicolaides, John D.: On the Free-Flight Motion of Missiles Having Slight Configurational Asymmetries. Rep. 858, Ballistic Res. Labs., 1953.

7. Seiff, Alvin; Sommer, Simon C.; and Canning, Thomas N.: Some Experiments at High Supersonic Speeds on the Aerodynamic and Boundary-Layer Transition Characteristics of High-Drag Bodies of Revolution. NACA RM A56I05, 1957.

8. Allen, H. Julian: Motion of a Ballistic Missle Angularly Misaligned With the Flight Path Upon Entering the Atmosphere, and Its Effect Upon Aerodynamic Heating, Aerodynamic Loads, and Miss Distance. NACA TN 4048, 1957.

9. Rasmussen, Maurice L.; and Kirk, Donn B.: On the Pitching and Yawing Motion of a Spinning Symmetric Missile Governed by an Arbitrary Nonlinear Restoring Moment. NASA TN D–2135, 1964.

10. Malcolm, Gerald N.: Stability and Drag Characteristics at Mach Numbers of 10 and 26 of a Proposed Slender Atmospheric Probe. NASA TN D–3917, 1967.

11. McDevitt, John B.: An Exploratory Study of the Roll Behavior of Ablating Cones. AIAA Paper 70–562, 1970.

12. Chapman, Gary T.: Theoretical Laminar Convective Heat Transfer and Boundary-Layer Characteristics on Cones at Speeds to 24 Km/Sec. NASA TN D–2463, 1964.

13. Rasmussen, Maurice L.; and Kirk, Donn B.: A Study of Damping in Nonlinear Oscillations. NASA TR R–249, 1966.

14. Levy, Lionel L., Jr.; and Tobak, Murray: Nonlinear Aerodynamics of Bodies of Revolution in Free-Flight. AIAA Paper 70–205, 1970.

TABLE 1. – TEST DATA

Test	V, ft/sec	M	Re, $\times 10^{-6}$	C_D	$C_{m_{\alpha_l}}$	C_{L_α}	$C_{m_q} + C_{m_{\dot\alpha}}$	σ_m	σ_{min}	σ_{rms}	$\omega d/V$	P, $\times 10^{-3}$ deg/sec
(a) Plastic ablating models: d=0.35 in.; m=0.536 gm; X_{cg}=0.622 in.; I_y=2.71$\times 10^{-8}$ slug ft^2; I_x=2.75$\times 10^{-9}$ slug ft^2												
493	17807	15.7	0.31	0.149	−0.579	1.209	−2.15	9.63	0.71	6.61	0.006	−64.5
497	17236	15.2	.30	.139	−.499	1.035	.27	8.36	.96	5.91	.006	−97.6
538	17778	15.7	.32	.162	−.609	1.376	−2.19	11.20	1.60	7.79	.006	193.0
584	17116	15.2	.31	.143	−.546	1.098	−.58	8.51	1.50	6.03	.006	182.0
587	18160	16.1	.32	.124	−.271	.446	.69	5.00	1.94	3.68	.004	−138.0
591	18135	16.0	.32	.151	−.685	1.202	−1.72	9.80	1.88	6.80	.007	294.0
592	17947	15.9	.32	.242	−.725	1.761	−3.01	18.24	.04	13.08	.007	58.3
734	18136	16.1	.33	.154	−.638	1.281	−1.59	10.88	3.15	7.97	.007	333.0
735	18326	16.2	.33	.131	−.464	1.056	−1.28	7.18	.40	5.00	.006	44.0
737	18190	16.1	.33	.123	−.251	.647	−.08	4.57	2.79	3.84	.004	337.0
738	18133	16.1	.33	.129	−.382	.855	.19	6.28	2.51	4.85	.005	−327.0
(b) Metal nonablating models: d=0.35 in.; m=1.341 gm; X_{cg}=0.618 in.; I_y=7.92$\times 10^{-8}$ slug ft^2; I_x=6.63$\times 10^{-9}$ slug ft^2												
595	16270	14.5	.29	.145	−.536	1.203	−2.70	7.09	.40	5.31	.004	−.7
654	16786	14.8	.30	.131	−.398	.948	−3.63	5.84	.95	4.15	.003	52.5
655	17309	15.3	.30	.224	−.648	1.600	−4.37	15.91	.79	11.35	.004	23.3
656	17266	15.3	.30	.327	−.660	1.783	−4.63	22.59	1.38	16.26	.004	34.4
657	17156	14.9	.29	.304	−.677	1.682	−5.28	20.76	1.56	14.67	.004	−.5

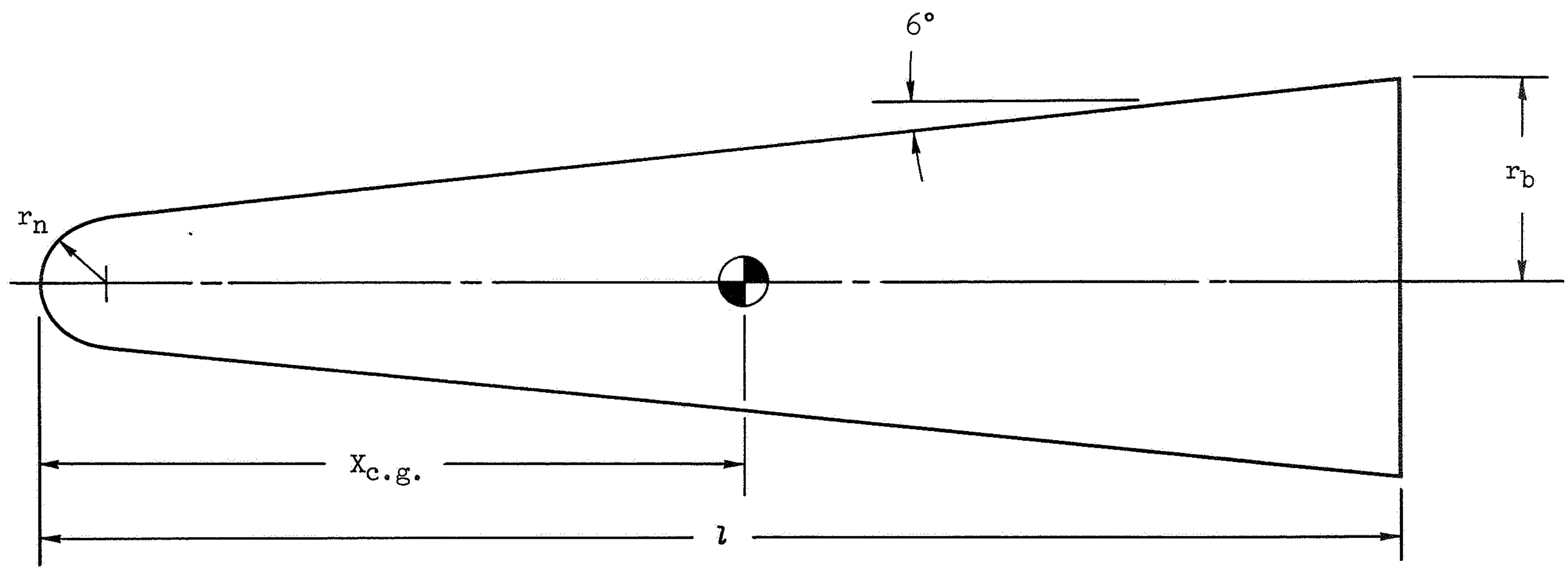

$$\frac{r_n}{r_b} = 0.31, \quad \frac{X_{c.g.}}{l} = 0.52$$

Figure 1.- Model configuration.

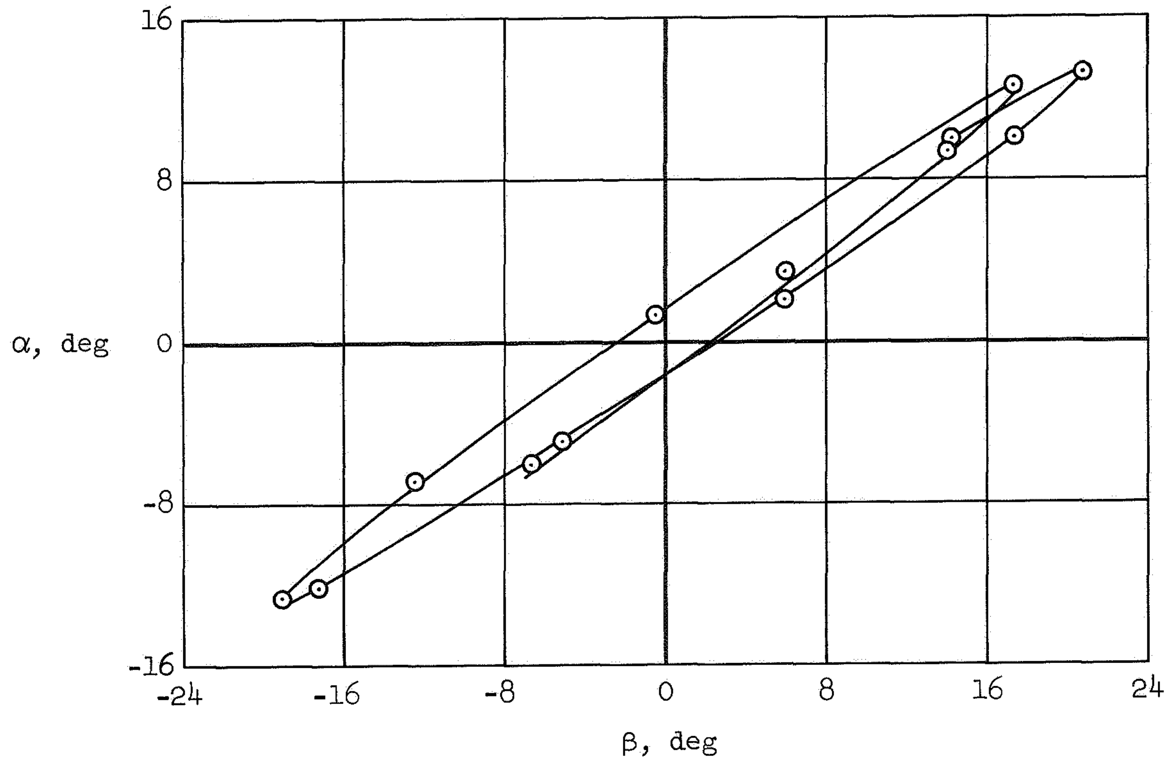

(a) Nonablating model

Figure 2.- Typical pitch-yaw motions.

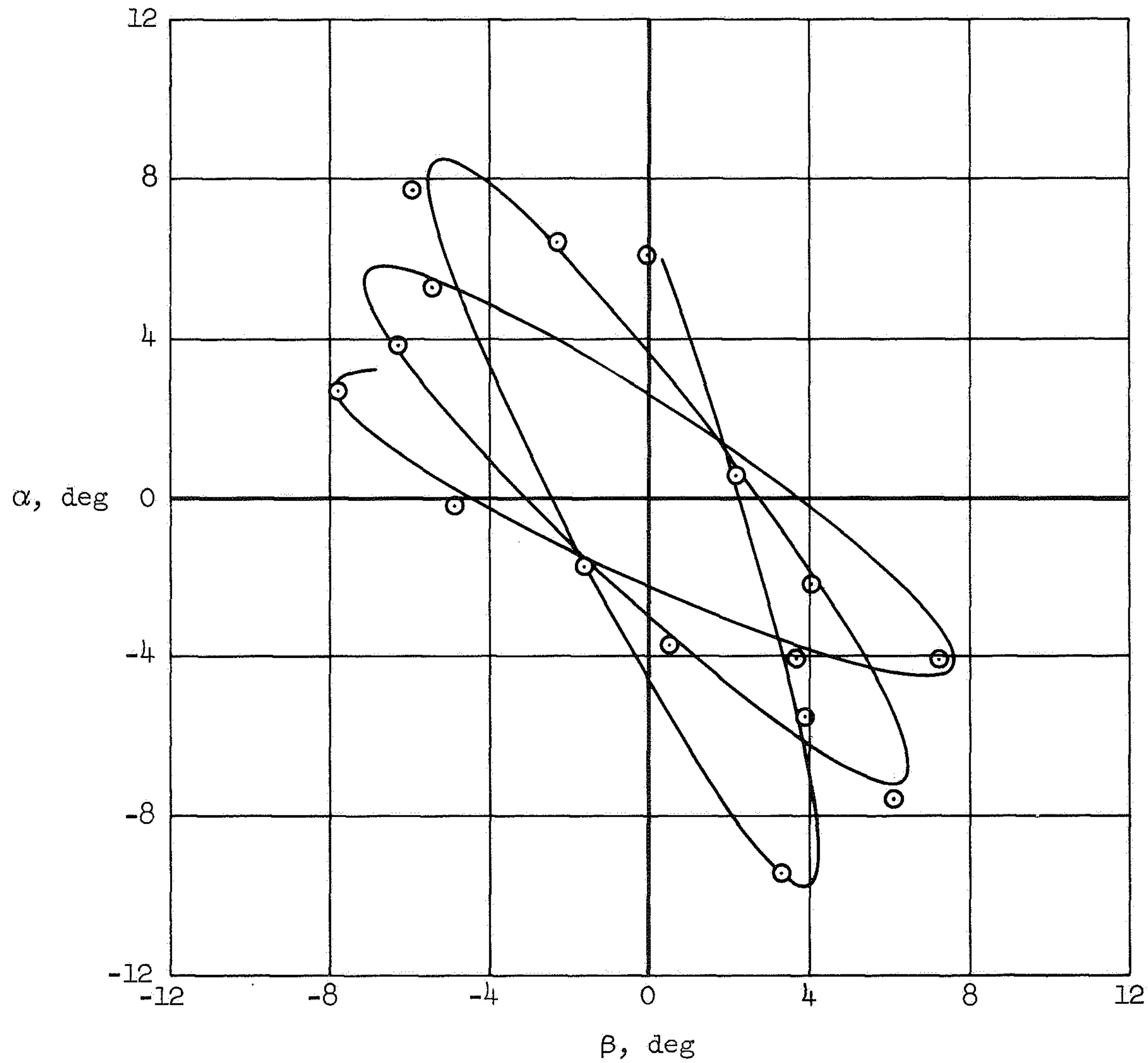

(b) Ablating model

Figure 2.- Concluded.

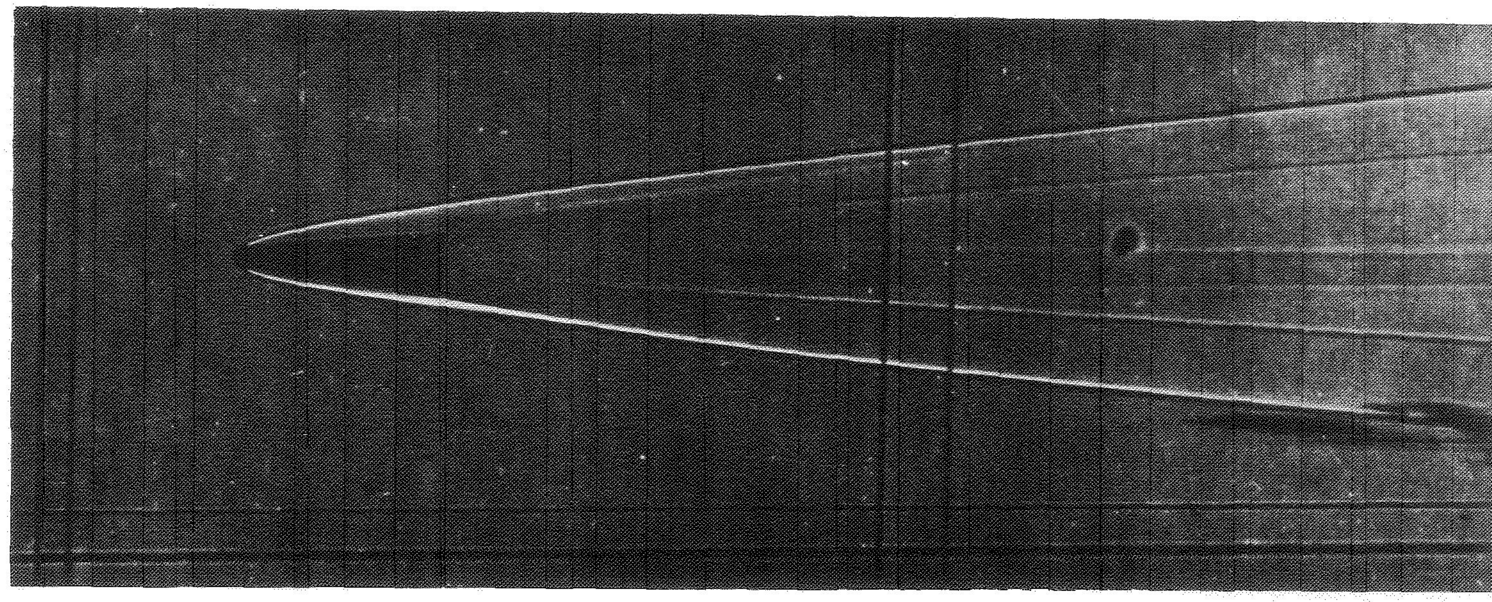

(a) Nonablating metal model; $\alpha = 1.3^\circ$ ($\beta = 5.5^\circ$).

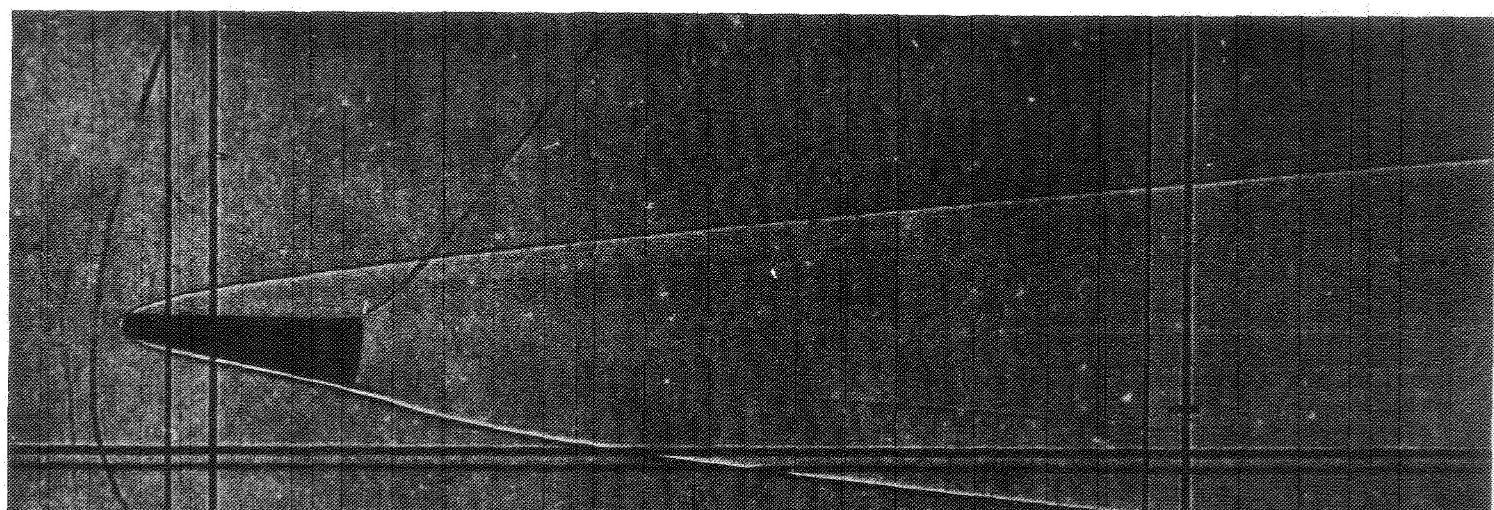

(b) Ablating plastic model; $\alpha = 7.7^\circ$ ($\beta = 5.9^\circ$).

Figure 3.— Shadowgraphs of model in flight; $M \approx 15$.

	Theory		Experiment	
	No ablation	Ablation	No ablation	Ablation
Wave drag (Rakich) Skin friction Base drag Viscous interaction	0.088 0.020 0.003 0.012	Same 0.005 Same 0.018		
Total drag (α = 0°)	0.123	0.114	0.120	0.113

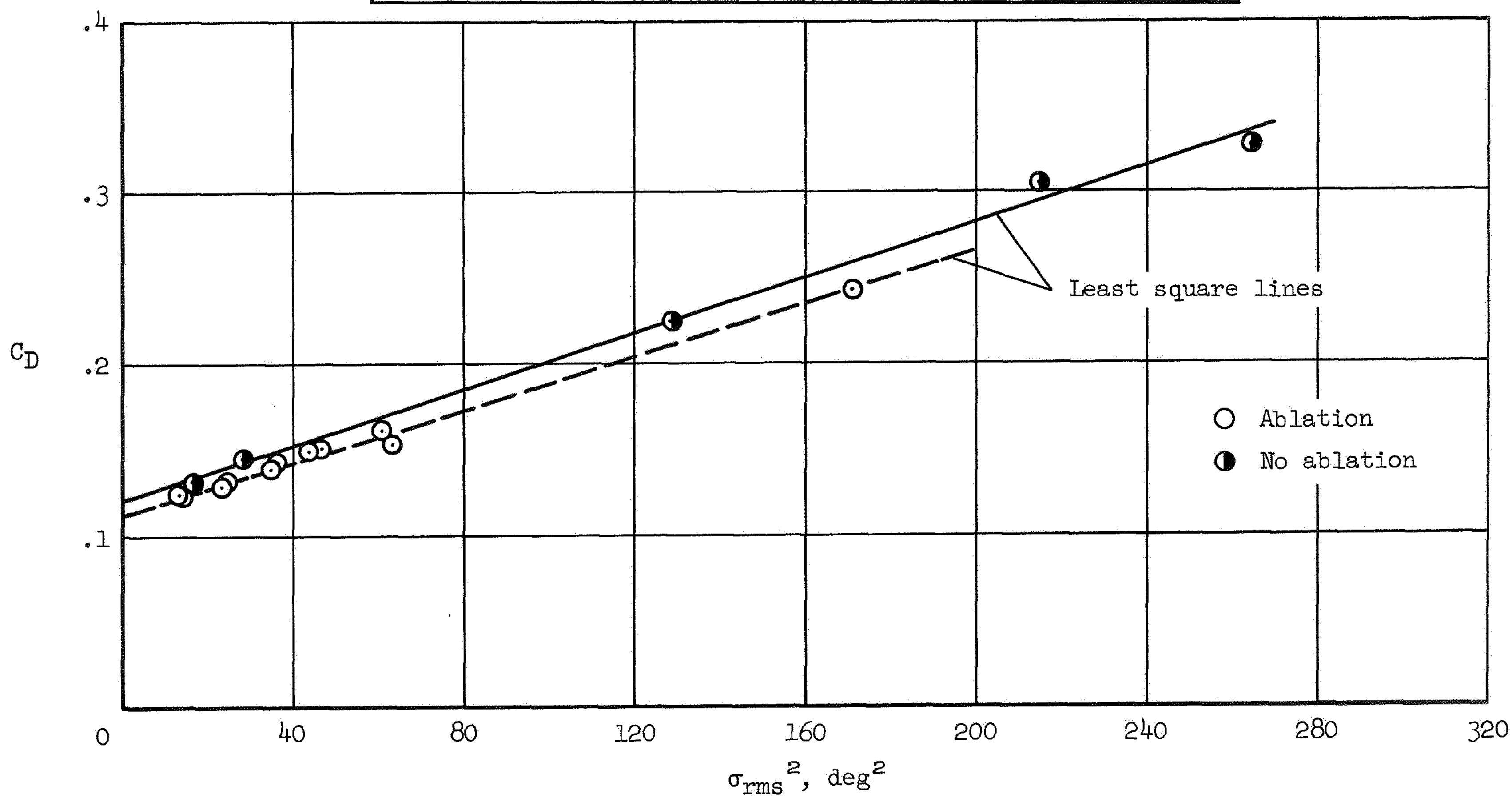

Figure 4.- Drag coefficient versus mean square resultant angle of attack; M ≈ 15, Re ≈ 0.3×10^6.

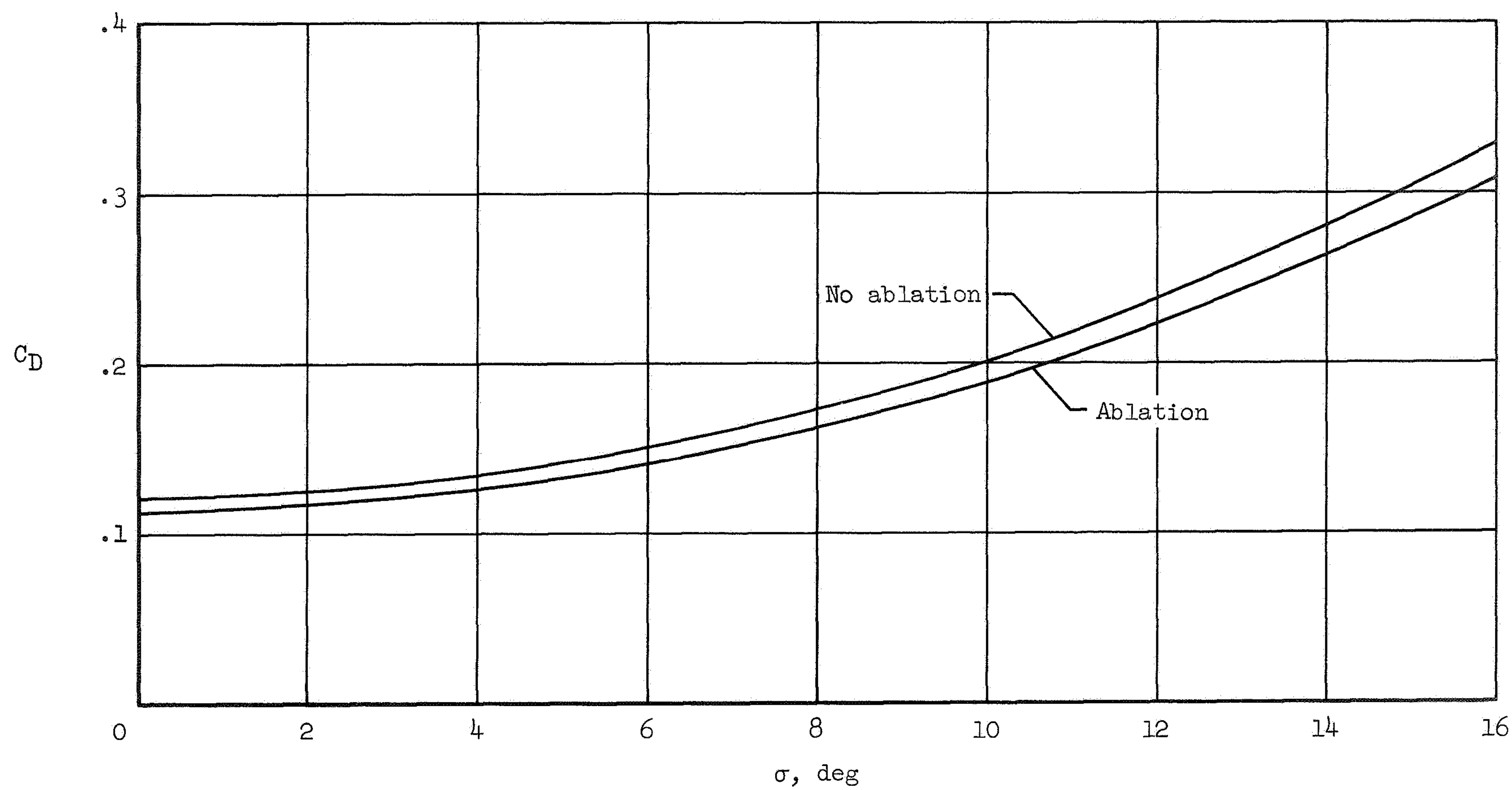

Figure 5.- Drag coefficient versus resultant angle of attack.

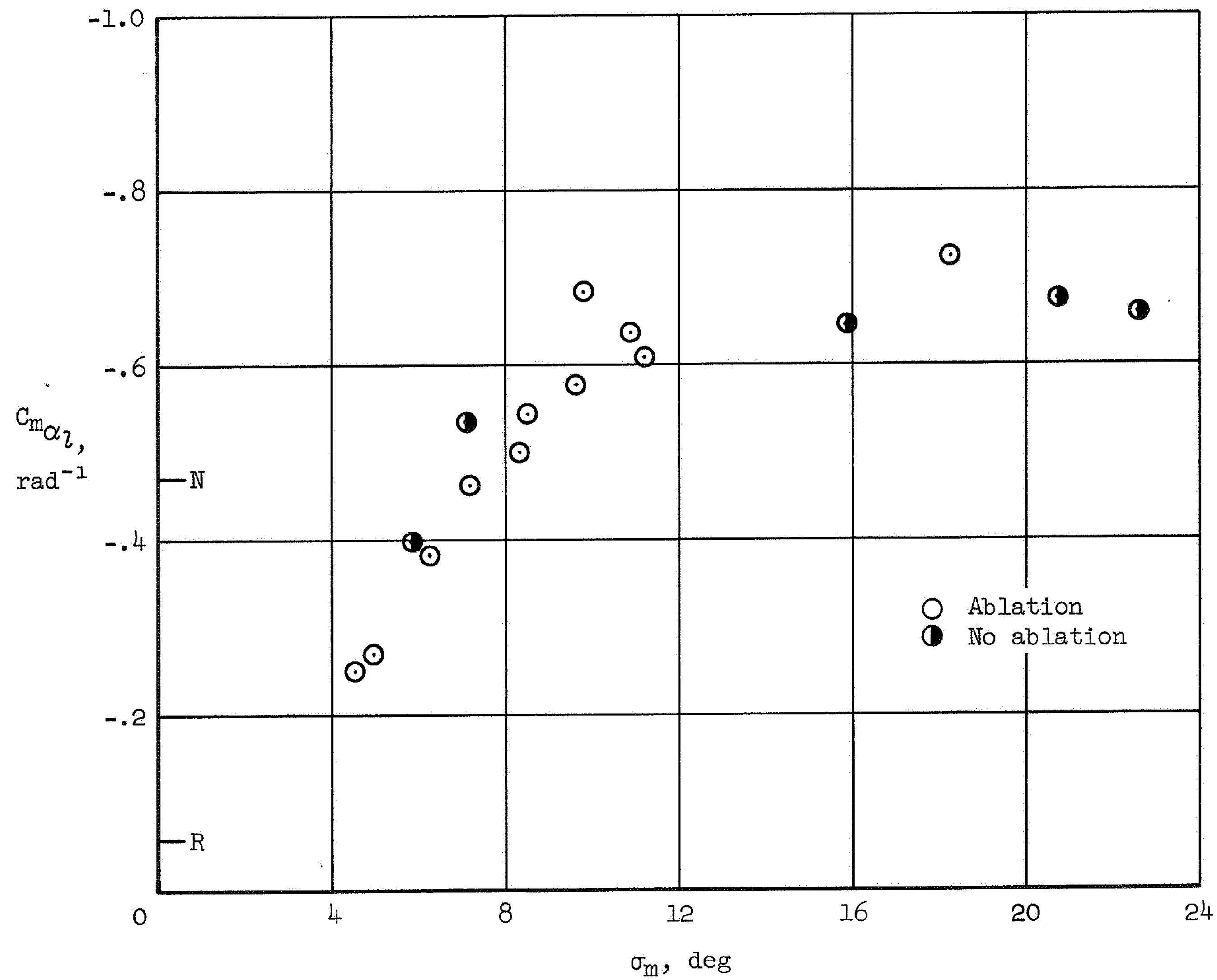

Figure 6.- Static stability coefficient versus average maximum resultant angle of attack; $M \approx 15$, $Re \approx 0.3 \times 10^6$, $X_{c.g.}/l = 0.52$.

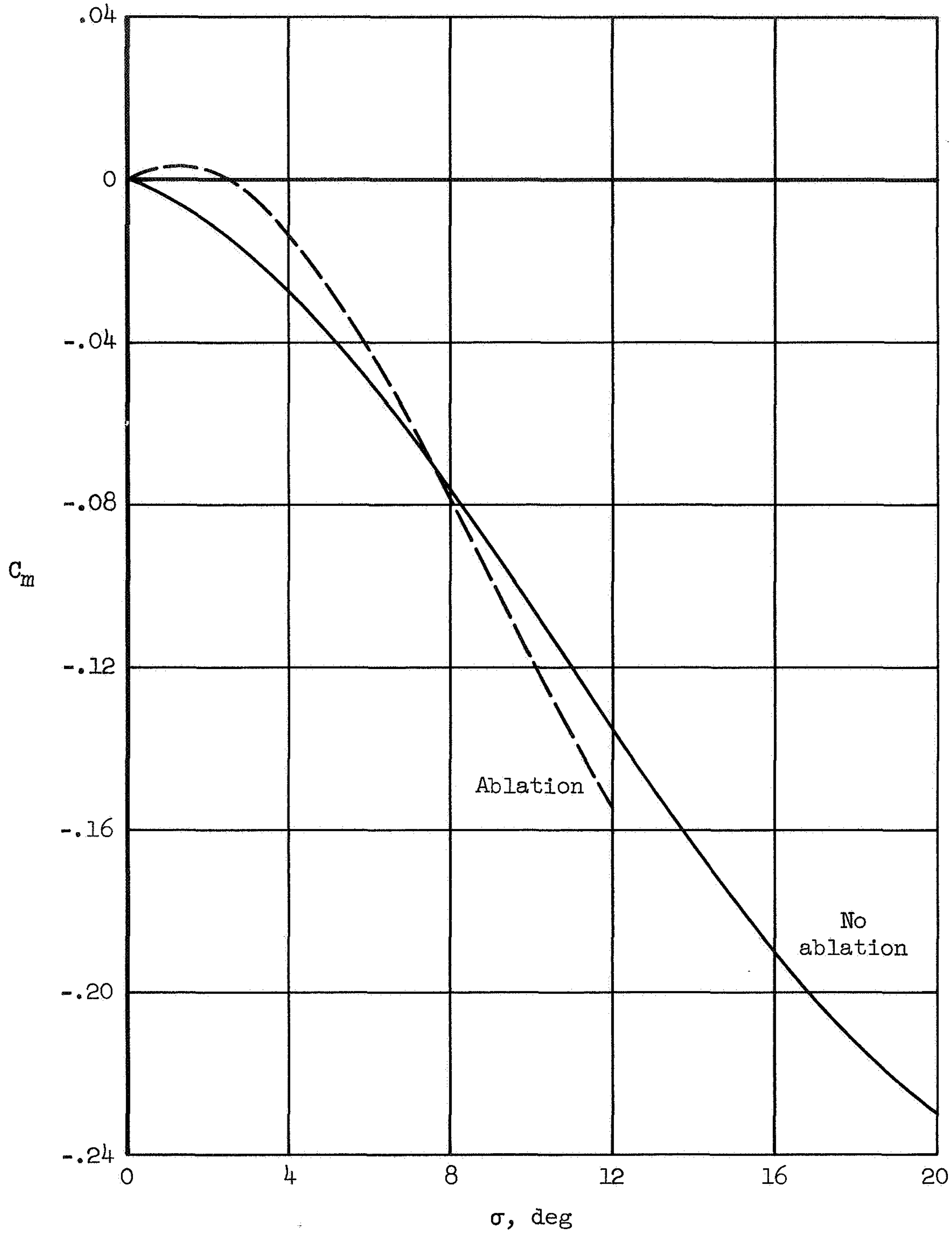

Figure 7.- Pitching moment versus resultant angle of attack.

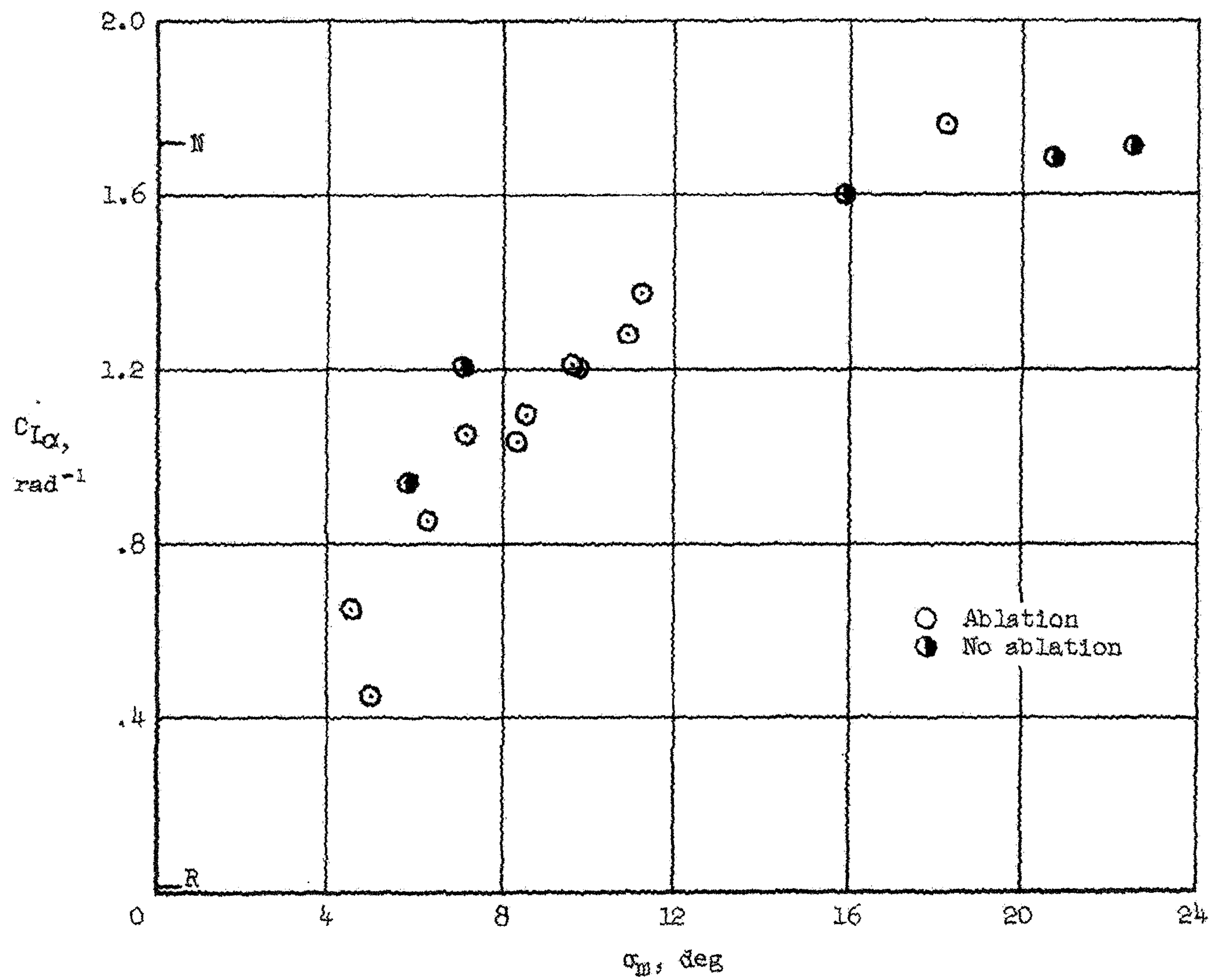

Figure 8.- Lift curve slope versus average maximum resultant angle of attack; $M \approx 15$, $Re \approx 0.3X10^6$.

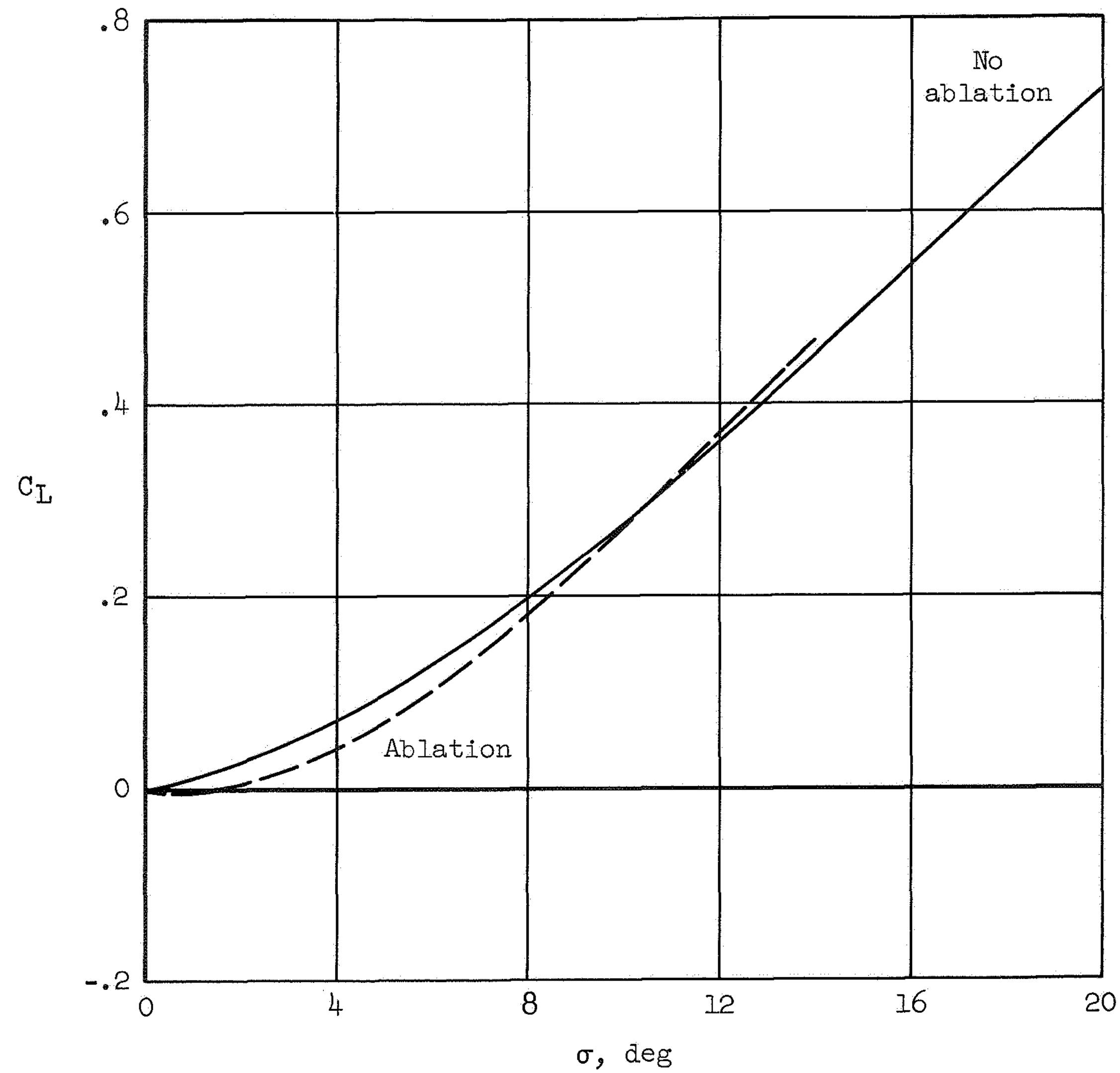

Figure 9.- Lift coefficient versus resultant angle of attack.

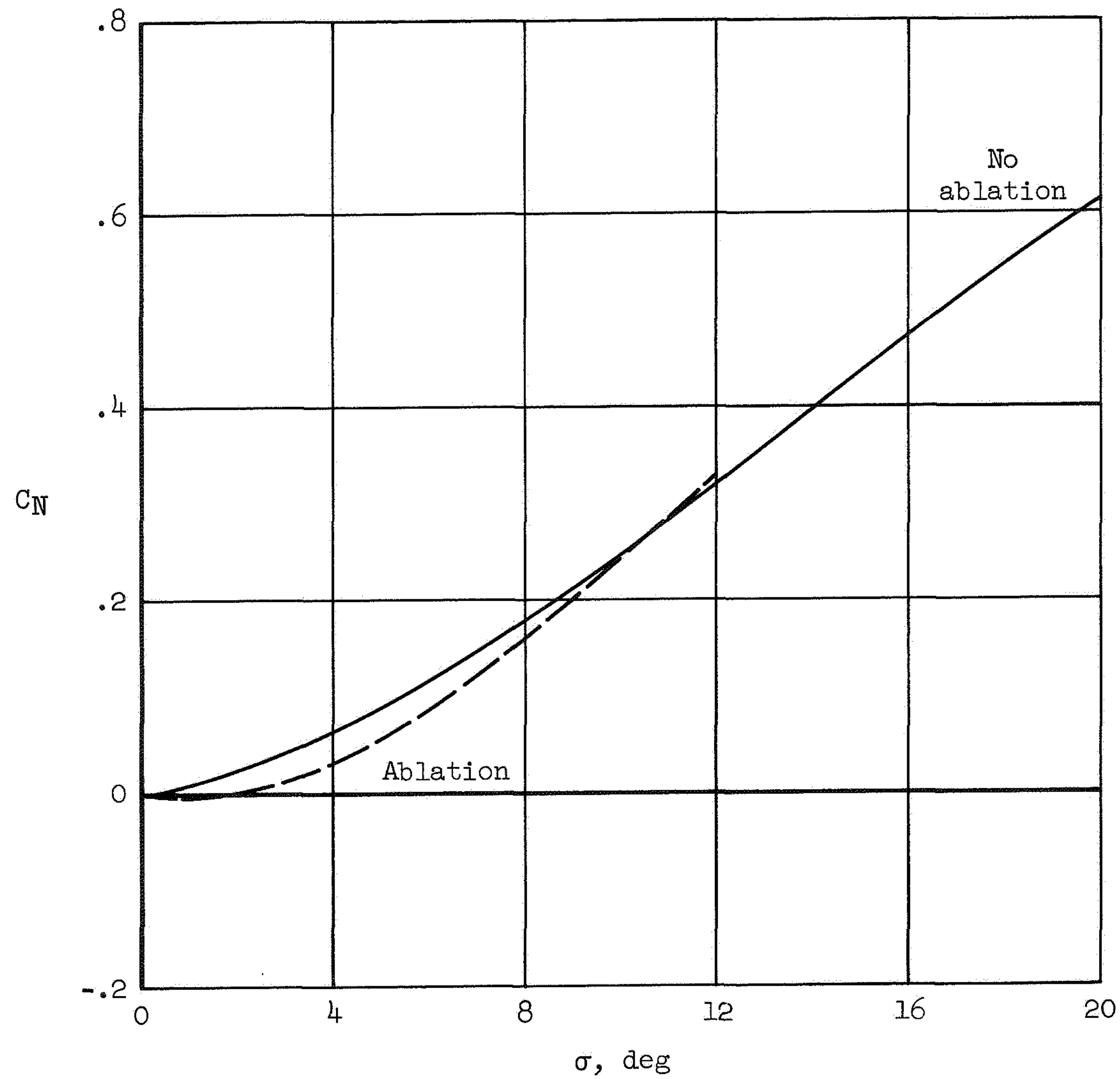

Figure 10.- Normal force coefficient versus resultant angle of attack.

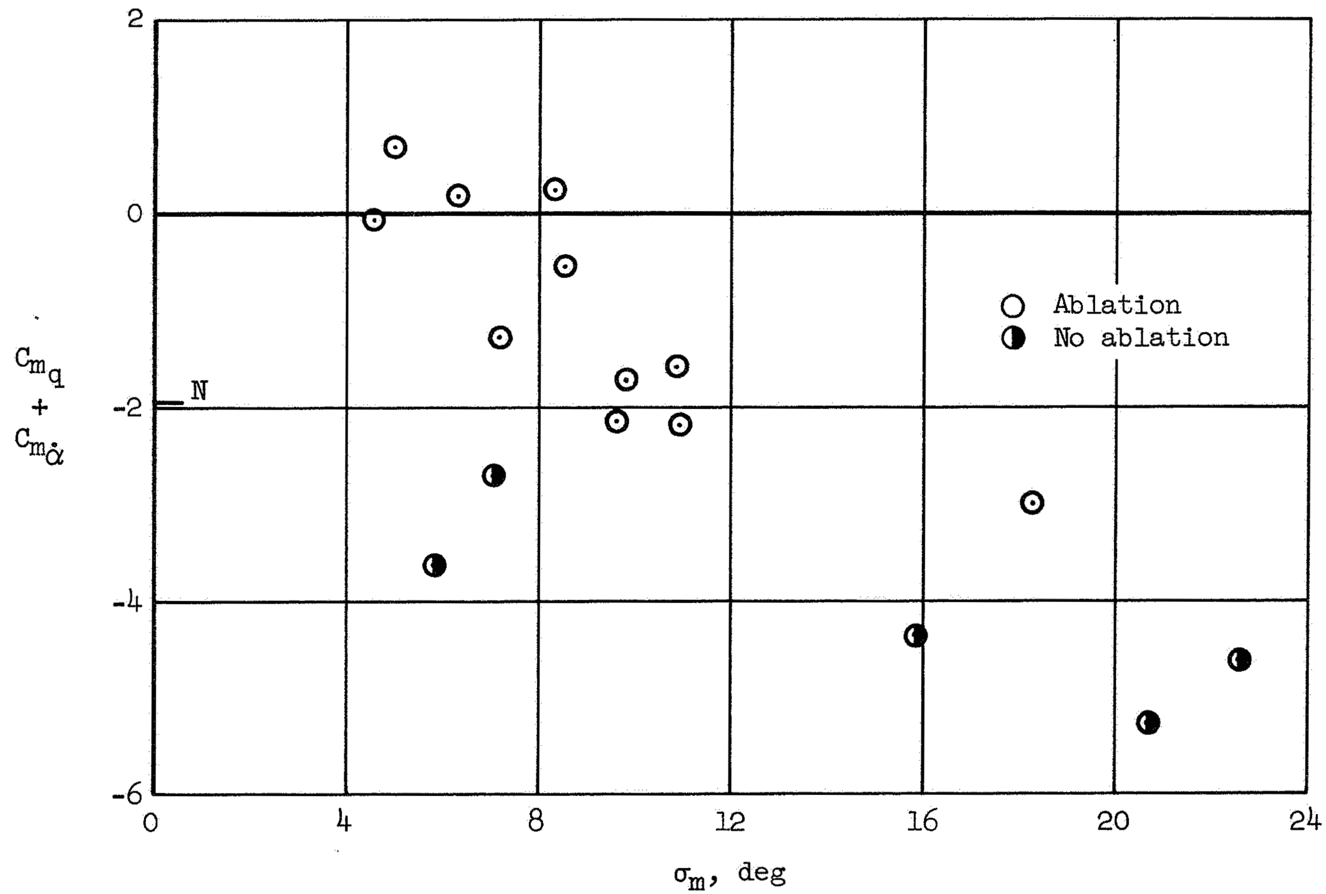

Figure 11.- Damping-in-pitch derivative versus average maximum resultant angle of attack; $M \approx 15$, $Re \approx 0.3 \times 10^6$, $X_{c.g.}/l = 0.52$, $\omega d/V \approx 0.003 - 0.007$.

NASA-Langley, 1973 —— 1 A–4558

"The aeronautical and space activities of the United States shall be conducted so as to contribute . . . to the expansion of human knowledge of phenomena in the atmosphere and space. The Administration shall provide for the widest practicable and appropriate dissemination of information concerning its activities and the results thereof."

—NATIONAL AERONAUTICS AND SPACE ACT OF 1958

NASA SCIENTIFIC AND TECHNICAL PUBLICATIONS

TECHNICAL REPORTS: Scientific and technical information considered important, complete, and a lasting contribution to existing knowledge.

TECHNICAL NOTES: Information less broad in scope but nevertheless of importance as a contribution to existing knowledge.

TECHNICAL MEMORANDUMS: Information receiving limited distribution because of preliminary data, security classification, or other reasons. Also includes conference proceedings with either limited or unlimited distribution.

CONTRACTOR REPORTS: Scientific and technical information generated under a NASA contract or grant and considered an important contribution to existing knowledge.

TECHNICAL TRANSLATIONS: Information published in a foreign language considered to merit NASA distribution in English.

SPECIAL PUBLICATIONS: Information derived from or of value to NASA activities. Publications include final reports of major projects, monographs, data compilations, handbooks, sourcebooks, and special bibliographies.

TECHNOLOGY UTILIZATION PUBLICATIONS: Information on technology used by NASA that may be of particular interest in commercial and other non-aerospace applications. Publications include Tech Briefs, Technology Utilization Reports and Technology Surveys.

Details on the availability of these publications may be obtained from:

SCIENTIFIC AND TECHNICAL INFORMATION OFFICE

NATIONAL AERONAUTICS AND SPACE ADMINISTRATION

Washington, D.C. 20546